

Article

Oleocanthal Ameliorates Metabolic and Behavioral Phenotypes in a Mouse Model of Alzheimer's Disease

Euitaek Yang¹, Junwei Wang¹, Lauren N. Woodie² , Michael W. Greene²  and Amal Kaddoumi^{1,*} 

¹ Department of Drug Discovery and Development, Harrison College of Pharmacy, Auburn University, 720 S Donahue Dr., Auburn, AL 36849, USA; ezy0014@auburn.edu (E.Y.); jzw0164@auburn.edu (J.W.)

² Department of Nutrition, College of Human Sciences, Auburn University, Auburn, AL 36849, USA; lauren.woodie@pennmedicine.upenn.edu (L.N.W.); mwg0006@auburn.edu (M.W.G.)

* Correspondence: kaddoumi@auburn.edu

Abstract: Aging is a major risk factor for Alzheimer's disease (AD). AD mouse models are frequently used to assess pathology, behavior, and memory in AD research. While the pathological characteristics of AD are well established, our understanding of the changes in the metabolic phenotypes with age and pathology is limited. In this work, we used the Promethion cage systems[®] to monitor changes in physiological metabolic and behavioral parameters with age and pathology in wild-type and 5xFAD mouse models. Then, we assessed whether these parameters could be altered by treatment with oleocanthal, a phenolic compound with neuroprotective properties. Findings demonstrated metabolic parameters such as body weight, food and water intake, energy expenditure, dehydration, and respiratory exchange rate, and the behavioral parameters of sleep patterns and anxiety-like behavior are altered by age and pathology. However, the effect of pathology on these parameters was significantly greater than normal aging, which could be linked to amyloid- β deposition and blood–brain barrier (BBB) disruption. In addition, and for the first time, our findings suggest an inverse correlation between sleep hours and BBB breakdown. Treatment with oleocanthal improved the assessed parameters and reduced anxiety-like behavior symptoms and sleep disturbances. In conclusion, aging and AD are associated with metabolism and behavior changes, with the changes being greater with the latter, which were rectified by oleocanthal. In addition, our findings suggest that monitoring changes in metabolic and behavioral phenotypes could provide a valuable tool to assess disease severity and treatment efficacy in AD mouse models.

Keywords: Alzheimer's disease; blood–brain barrier; metabolic phenotype; sleep behavior; Promethion cages; oleocanthal



check for updates

Citation: Yang, E.; Wang, J.; Woodie, L.N.; Greene, M.W.; Kaddoumi, A. Oleocanthal Ameliorates Metabolic and Behavioral Phenotypes in a Mouse Model of Alzheimer's Disease. *Molecules* **2023**, *28*, 5592. <https://doi.org/10.3390/molecules28145592>

Academic Editor: José Marco-Contelles

Received: 12 June 2023
Revised: 15 July 2023
Accepted: 21 July 2023
Published: 23 July 2023



Copyright: © 2023 by the authors. Licensee MDPI, Basel, Switzerland. This article is an open access article distributed under the terms and conditions of the Creative Commons Attribution (CC BY) license (<https://creativecommons.org/licenses/by/4.0/>).

1. Introduction

Alzheimer's disease (AD) is a neurodegenerative disorder causing dementia. Age is considered a major risk factor for developing AD. Aging alters many physiological processes in the human body and metabolic and behavioral phenotypes [1]. Metabolic and behavioral phenotyping is used to assess alterations in physiological metabolism and behavior that are affected by numerous factors, including diet, lifestyle, disease conditions, and other environmental factors [2]. Examples of metabolic and behavioral phenotypes that are affected by age and disease include food and water intake, activity, movement, energy expenditure, respiratory exchange, hydration, and sleep patterns [3].

While the pathological characteristics of AD are well established, our understanding of the changes in the metabolic phenotypes with age and pathology continues to be limited. Several studies have reported appetite loss in persons with mild cognitive impairment (MCI) and dementia [4]. Decreased meal consumption could result in malnutrition, dehydration, failing of body homeostasis, weakening of immunity, and reduction in cognitive function [5]. In AD patients, a range of factors can affect appetite, including fastidiousness in eating and the inability to feel hungry because of brain atrophy, disturbance of eating

behavior, loss of the ability to use eating utensils, and decrease in swallowing function [6]. A change in food intake could affect other metabolic parameters, such as activity and energy consumption [7]. In addition, AD patients experience sleep disturbances that may precede the other clinical signs of AD [8]. Sleep disorders may affect the circadian rhythm, which has been linked to fluctuations in amyloid- β ($A\beta$) levels in interstitial brain fluid (ISF) and cerebrospinal fluid (CSF) [9–12]. In the adult brain, the clearance of $A\beta$ during sleep is two-fold faster than during wakefulness [13], and brain $A\beta$ accumulation induces excessive daytime sleepiness [14]. In humans, monitoring the sleep–wake cycle in individuals with AD aged 45–75 years has shown a decreased sleep efficiency and increased nap frequency in individuals with $A\beta$ deposition compared with individuals of the same age but without $A\beta$ deposition as determined by CSF- $A\beta_{42}$ level [15]. Thus, AD could affect the sleep pattern, and at the same time, sleep disturbances might contribute to AD progression [8]. Besides sleep disturbances, anxiety is one of the neuropsychiatric symptoms of AD [16]. Anxiety has also been considered a risk factor for AD, especially in midlife [17]. AD patients exhibit anxiety at the MCI stage, which is associated with an increased likelihood of dementia [18].

AD research frequently uses mouse models to understand the pathology and behavior and test potential treatments. Studies investigating mitochondrial respiratory function, circadian-related proteins, eye movement, and electroencephalography are often used to test the pathology effect on metabolism and circadian rhythms in mice [19–23]. Open field, elevated plus-maze, and light/dark tests have been used for anxiety-like behavior [18]. These methodologies are performed in brain tissues or require mouse restraining or training, which could introduce a stress factor that could confound the results.

Promethion cage systems[®] are a valuable tool for metabolic and behavioral phenotyping that simultaneously monitors metabolic data with behavioral events under natural conditions without introducing a stress factor to the animals. Examples of metabolic and behavior parameters that these systems could obtain include body weight, food and water intake, movement, energy expenditure, dehydration level, and respiratory exchange. Based on the mouse behavior and movement monitored by sensors in the cages, sleep pattern and anxiety-like behavior could be determined (Table 1).

Table 1. A summary of the assessed metabolic parameters with their abbreviations.

Parameters	Definition
Body weight	Mean body mass of the animal, in grams (g)
Food intake	Mass of food consumed by animal, in gram (g)
Water intake	Mass of water consumed by animal, in gram (g)
EE	Mean energy expenditure, in kcal/h
VCO ₂	Mean rate of carbon dioxide emission, in mL/min
VO ₂	Mean rate of oxygen consumption in mL/min
RER	Respiratory exchange ratio, VCO ₂ /VO ₂ , unit-less
VH ₂ O	Mean rate of water vapor loss, in mL/min
Distance travelled	Sum of all distances traveled, in meters
Cumulative distance	Sum of cultivating distance traveled, in meters
Sleep	Sleep time (h) = quiet for > 40 s

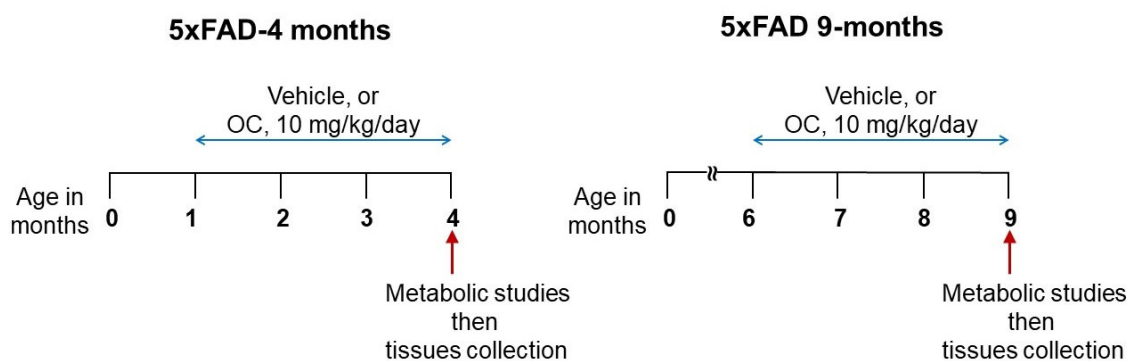
In this work, we aimed to utilize the Promethion cage system to compare differences in metabolic and behavioral parameters as a function of age (4 vs. 9 months) and pathology in wild-type (WT) and 5xFAD as a mouse model of AD and then to evaluate whether the assessed metabolic and behavioral phenotypes respond to oleocanthal (OC) as a treatment for AD. OC is a naturally occurring phenolic secoiridoid isolated from extra-virgin olive oil (EVOO), which possesses anti-inflammatory effects similar to the nonsteroidal anti-inflammatory drug ibuprofen [24]. Studies from our laboratory have reported the beneficial effect of OC in AD mouse models where OC treatment reduced brain $A\beta$ levels, improved the blood–brain barrier (BBB) function, reduced neuroinflammation, enhanced autophagy, and improved memory function [25–28].

We demonstrate here that age and pathology are associated with sleep disturbances, altered energy expenditure, activity rate, and moved distances associated with anxiety-like behavior. Between the two age groups, 9-month-old mice demonstrated greater differences in the monitored parameters than the younger group. Furthermore, our results indicate that 5xFAD mice treated with OC, 10 mg/kg, improved several of the assessed parameters to levels similar to or approaching those of the WT mice. Our findings suggest that metabolic and behavioral phenotypes are altered with age and pathology and support their use to monitor disease progression, severity, and treatment response as an additional approach to conventional currently used approaches.

2. Results

2.1. Effect of Age on the Phenotypic Parameters in WT and 5xFAD Mice

A schematic diagram of the animals' experimental design is presented in Scheme 1. The metabolic phenotype parameters were measured over a 24 h period starting at zeitgeber time (ZT) 0 (6 am). ZT0 represents lights on, and ZT12 represents lights off. All assessed parameters are summarized in Table 1.



Scheme 1. A schematic diagram of the experimental design. Four- and nine-month-old. WT mice received only the vehicle.

Figures S1 and S2 (Supplementary data) show the effect of age (4 vs. 9 months) on assessed parameters in WT and 5xFAD mice, respectively, over the 24 h diurnal rhythm time. Tables S1 and S2 list the significance of the difference of each parameter at each time point for WT and 5xFAD mice, respectively. As shown in Figure S1 and Table S1, as expected, a gain in body weight was observed with normal aging. In addition, time points comparison of the parameters demonstrated a significant reduction in mean energy expenditure (EE), the mean rate of carbon dioxide emission (VCO_2), the mean rate of oxygen consumption (VO_2), respiratory exchange ratio (RER), and mean rate of water vapor loss (VH_2O) in WT-9-month-old (WT-9m) mice compared to WT-4-month-old (WT-4m) mice across multiple time points in the ZT. On the other hand, in 5xFAD mice, except for the VH_2O (at daytime and nighttime), distance traveled (meters), and cumulative distance traveled (mainly nighttime) showed a significant increase with aging. However, monitored changes of other assessed parameters over time between 0–24 h did not show significant alteration between 4-(5xFAD-4m) and 9-(5xFAD-9m) month-old mice (Figure S2 and Table S2).

Figure 1 demonstrates the 12 h circadian (day/night) data for the effect of age and pathology on the parameters at day (average of ZT0–11) and night (average of ZT12–23) times. As shown in Figure 1A, in WT and 5xFAD mice, 9-month-old mice have higher body weight than the 4-month-old mice. WT-9m mice exhibited a significant body weight gain by 22% more than WT-4m, an effect not observed in 5xFAD mice where 4- and 9-month-old mice exhibited similar body weight (about 27 g). During the daytime, no significant difference was observed between WT-4m and WT-9m mice in food intake (Figure 1B), VH_2O (Figure 1H), and distance traveled (total and accumulative distance; Figure 1I,J), while a significant increase in water intake was observed (Figure 1C). However, the data demonstrated a significant reduction in EE, VCO_2 , VCO_2 , and RER parameters (Figure 1D–G) in

WT-9m compared to WT-4m mice. At nighttime, the older WT mice significantly reduced EE, VCO_2 , VO_2 , and VH_2O compared to the young mice (Figure 1D–F,H). In 5xFAD mice, with age, at daytime, a significant increase in food and water intake, VH_2O , and cumulative distance traveled were observed (Figure 1B,C,H,I). At nighttime, 5xFAD-9m mice demonstrated a significant increase in VH_2O and cumulative distance traveled compared to 5xFAD-4m mice (Figure 1H,J). These results suggest that aging in WT mice is associated with reduced metabolic activity, while 5xFAD demonstrated either a no change or an increase in metabolic activity with aging.

2.2. Effect of Pathology on the Phenotypic Parameters at 4 and 9 Months in 5xFAD

Figures S3 and S4 demonstrate the effect of pathology on assessed parameters over time in WT and 5xFAD mice at 4 and 9 months of age, respectively. At 4 months, 5xFAD-4m mice demonstrated a significant reduction in the VH_2O parameter during the 24 h (Figure S3H). While there was a significant increase or a trend for an increase in the metabolic parameters at a few time points between ZT12–23 h (Figure S3, Table S3), which was better demonstrated in the daytime and nighttime data shown in Figure 1. On the other hand, compared to WT mice, at the age of 9 months, 5xFAD mice demonstrated a significant increase in all assessed metabolic parameters almost at all time points between ZT0–23 (Figure S4, Table S4), suggesting a significant pathology effect in older mice.

Regarding the effect of pathology on body weight, there was no significant difference between WT-4m and 5xFAD-4m mice. However, 5xFAD-9m mice demonstrated a significantly lower body weight than WT-9m mice by 20%; 5xFAD-9m mice exhibited a body weight similar to the 4-month-old WT and 5xFAD mice (27 g), suggesting the impact of advanced pathology on body weight (Figure 1A). Within the daytime (Figure 1), while 5xFAD-4m mice demonstrated lower food intake than WT-4m mice, this difference was insignificant (Figure 1B). Water intake, however, was significantly lower in 5xFAD-4m than in WT-4m mice (Figure 1C). All other parameters were comparable to WT mice except for the VH_2O parameter, where 5xFAD-4m mice exhibited a significantly lower rate of water loss than WT-4m mice (Figure 1H). On the other hand, at 9 months of age, 5xFAD demonstrated a significant reduction in water intake and a significant increase in the metabolic parameters such as EE, VCO_2 , VO_2 , RER, distance traveled, and cumulative distance traveled (Figure 1D–H,I,J). At nighttime, however, 5xFAD-4m mice showed a significant increase in VCO_2 , RER, and distance traveled, associated with a significant reduction in VH_2O compared to WT-4m mice. Like the changes at 4 months, 9-month-old 5xFAD mice maintained a significant increase in the metabolic parameters EE, VCO_2 , VO_2 , RER, VH_2O , distance traveled, and cumulative distance traveled (Figure 1D–J). Changes in the metabolic parameters with pathology indicate an anxiety-like behavior characterized by restlessness (increased movement and moving distances), sweating (increased water loss, VH_2O), sleep disturbances, and rapid breathing (VO_2 , VCO_2 , and RER), which collectively suggest that compared to WT mice, 5xFAD mice exhibit an anxiety-like behavior.

2.3. Effect of Age and Pathology on Sleep Pattern in WT and 5xFAD Mice

The sleep parameter was assessed as the proportion of cycles when a mouse sleeps, that is, when a mouse stays quiet for more than 40 s. As shown in Figure 1K, consistent with the circadian biology of mice, sleeping time during the daytime was observed to be longer than the nighttime in both mouse models. Sleeping behavior was also influenced by age and pathology. At day and night times, 9-month-old WT and 5xFAD mice demonstrated a significantly lower sleeping time by approximately 35% compared to the 4-month-old mice. For the effect of pathology on sleeping duration, during the daytime, while 5xFAD demonstrated a reduction trend, the effect was not significant between the two mouse models at both ages; during the nighttime, however, younger and older 5xFAD mice slept about 40% fewer hours than the WT mice.

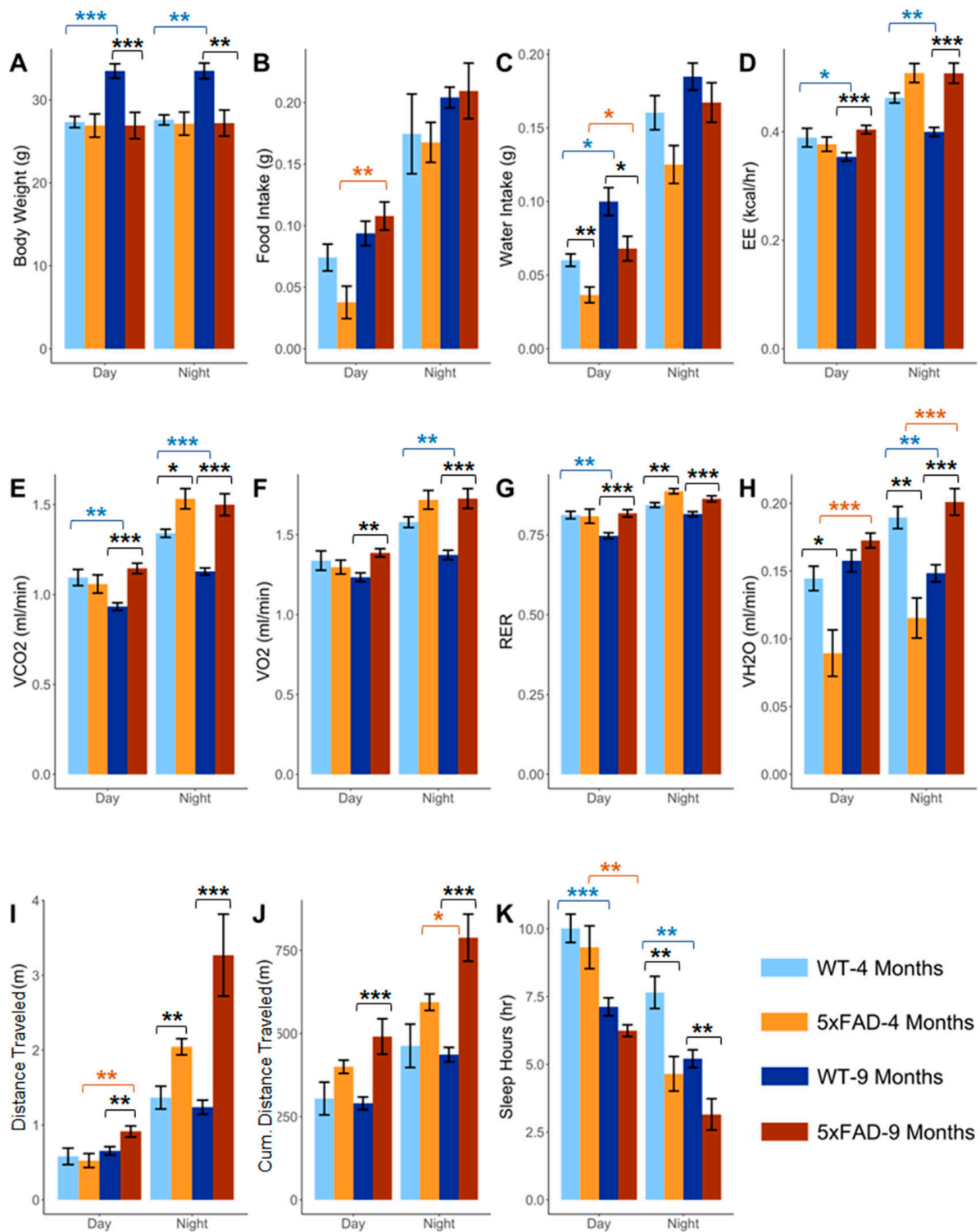


Figure 1. The effect of aging and pathology on the metabolic parameters (A) Body weight (g), (B) Food intake (g), (C) Water intake (g), (D) EE (kcal/h), (E) VCO₂ (mL/min), (F) VO₂ (mL/min), (G) RER, (H) VH₂O (mL/min), (I) Distance traveled (m), (J) Cumulative (Cum.) distance traveled (m), and (K) Sleep hours (h) in WT and 5xFAD mice at daytime and nighttime. The statistical significance is color-coded with blue stars indicating the difference in WT with age, orange stars indicating the difference in 5xFAD mice with age, and black stars indicating the difference between WT and 5xFAD mice. Data are presented as mean \pm SEM for $n = 10$ mice/group. * $p < 0.05$, ** $p < 0.01$, and *** $p < 0.001$.

2.4. Effect of Age and Pathology on BBB Function

In AD mouse models, extravasation of large molecular size proteins, such as IgG, is commonly observed [28,29]. Thus, IgG extravasation in mouse brains was assessed using immunofluorescence to evaluate the effect of age and pathology on BBB function. As shown in Figure 2, a significant IgG extravasation was observed in 5xFAD-9m mice. For the effect of age, while WT-9m demonstrated a trend of increase in IgG extravasation compared to the WT-4m mice, the effect was insignificant. In 5xFAD-9m mice, a significantly higher IgG extravasation was observed by 1.9-fold compared to 5xFAD-4m mice. For the effect of pathology, at both ages, 5xFAD mice demonstrated a significantly higher IgG, i.e., three-fold higher, extravasation than WT mice.

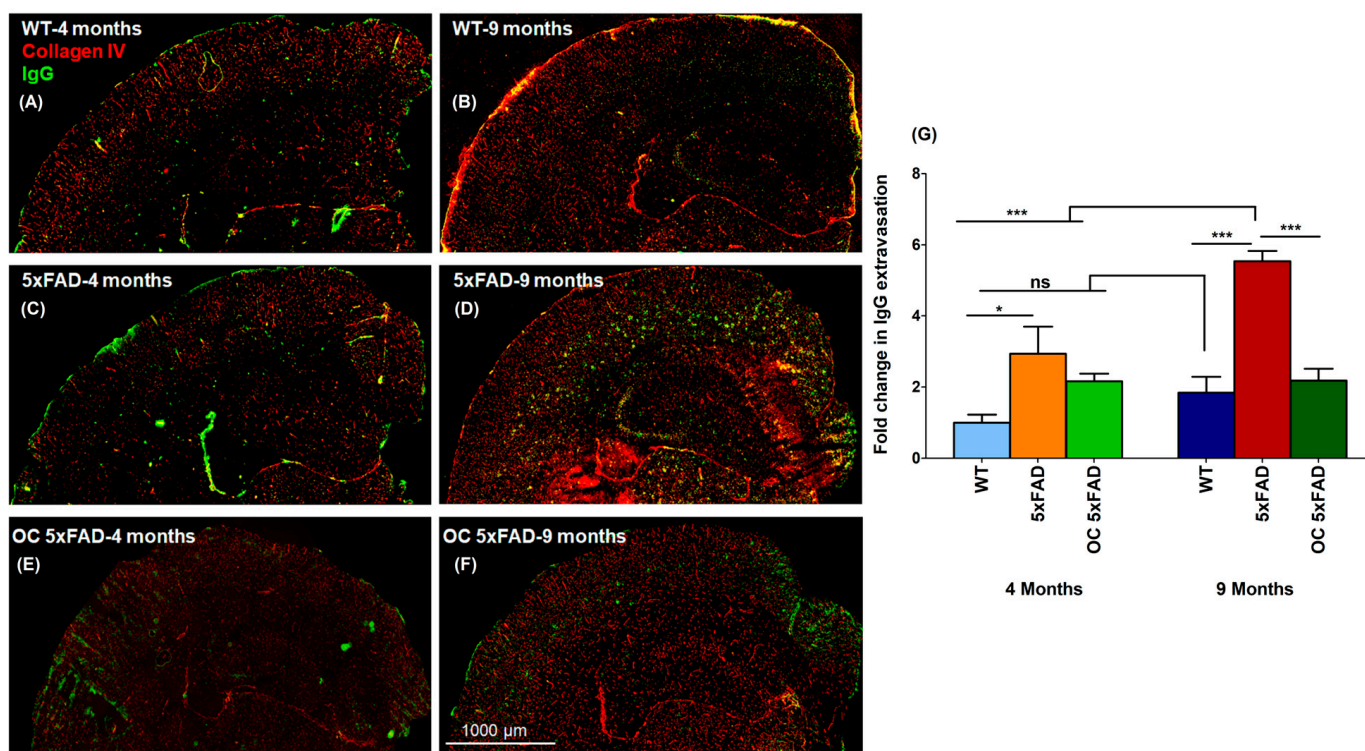


Figure 2. Representative brain sections stained with anti-mouse IgG antibody to detect IgG extravasation (green) and anti-collagen antibody (red) in mouse brain (A) WT-4-month-old, (B) WT-9-month-old, (C) 5xFAD-4-month-old, (D) 5xFAD-9-month-old, (E) 5xFAD-4-month-old treated with 10 mg/kg OC daily for 3 months, and (F) 5xFAD-9-month-old treated with 10 mg/kg OC daily for 3 months. (G) IgG optical density in mice brains was quantified for IgG extravasation. Data are presented as mean \pm SEM for $n = 5$ mice/group. ns for not significant, * $p < 0.05$, and *** $p < 0.001$ vs. WT-4 months WT mice. Scale bar, 1000 μ m.

2.5. Effect of Age and Pathology on Plasma and Brain $A\beta$ Levels in WT and 5xFAD Mice

Plasma and brain $A\beta_{40}$ and $A\beta_{42}$ levels were analyzed using ELISA. As shown in Figure 3A, for $A\beta_{40}$, there was a trend of increased plasma levels in 9-month-old compared to 4-month-old WT mice, but this increase was insignificant. On the other hand, for plasma $A\beta_{42}$, 9-month-old WT demonstrated two-fold higher levels than the 4-month-old mice (Figure 3B). Interestingly, 5xFAD-9m showed significantly lower $A\beta_{40}$ and $A\beta_{42}$ plasma levels by 74 and 70%, respectively, compared to the 5xFAD-4m mice. For the effect of pathology, at 4 months of age, the plasma levels of $A\beta_{40}$ and $A\beta_{42}$ in 5xFAD mice are 3- and 2.1-fold higher than in WT-4-month-old mice; as the mice aged, the plasma levels of $A\beta_{40}$ and $A\beta_{42}$ in 5xFAD-9-month-old mice were significantly lower than WT-9-month-old mice by 36% and 47%, respectively.

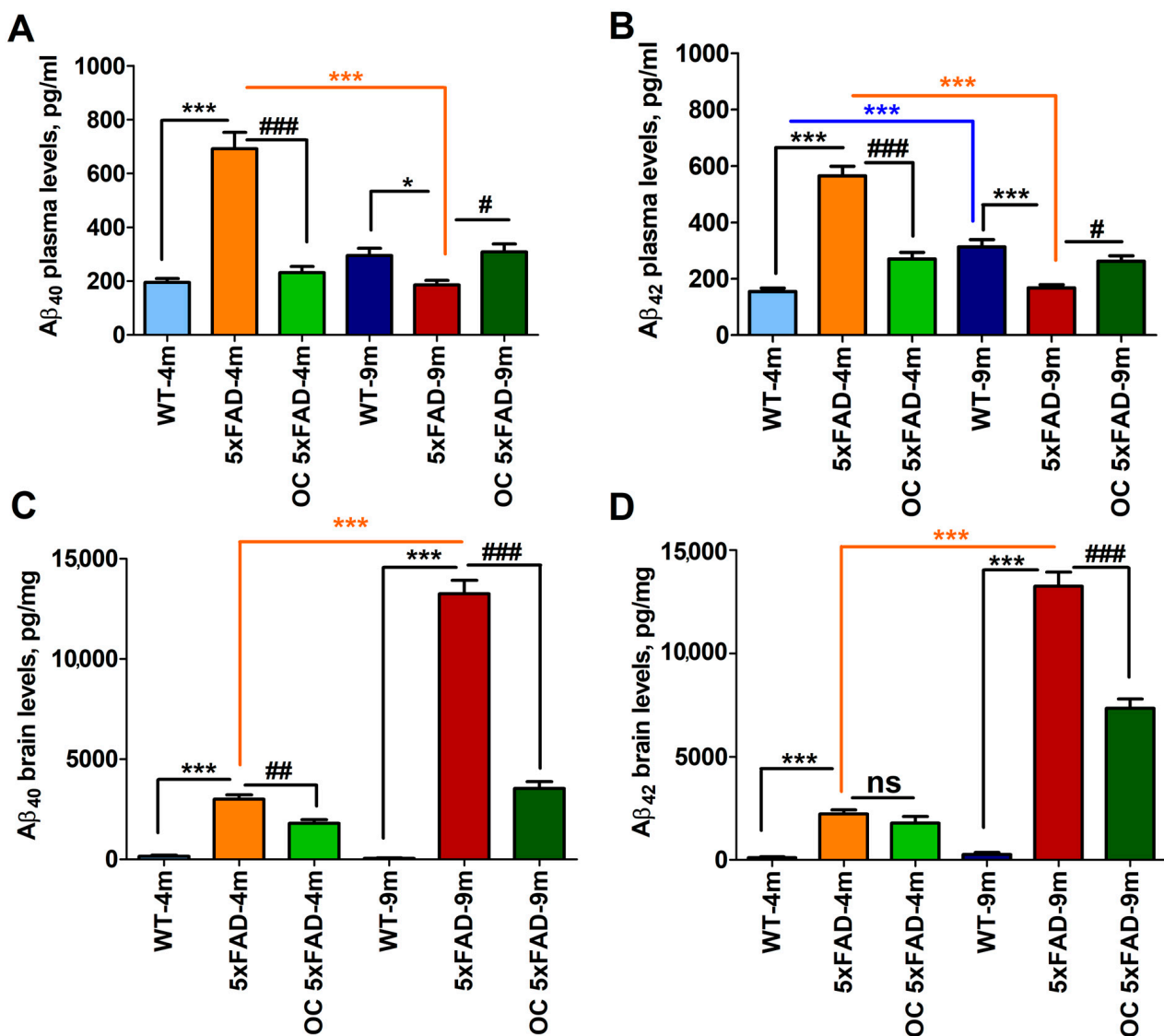


Figure 3. The effect of age, pathology, and 10 mg/kg OC treatment on levels of soluble plasma Aβ₄₀ (A) and Aβ₄₂ (B) and brain Aβ₄₀ (C) and Aβ₄₂ (D) as determined using ELISA in WT and 5xFAD mice. The statistical significance is color-coded with blue stars indicating the difference in WT with age, orange stars indicating the difference in 5xFAD mice with age, and black stars indicating the difference between WT and 5xFAD mice. Data are presented as mean ± SEM (*n* = 10/group). ns for not significant, * *p* < 0.05, *** *p* < 0.001, # *p* < 0.05, ## *p* < 0.01, and ### *p* < 0.001.

In the brain, as shown in Figure 3C,D, Aβ₄₀ and Aβ₄₂ levels in the 9-month-old 5xFAD were significantly higher than 4-month-old 5xFAD by 4.4- and 6.0-fold, respectively; at both ages, brain Aβ₄₀ and Aβ₄₂ levels in 5xFAD mice were significantly higher than the WT mice, which showed negligible levels of Aβ₄₀ and Aβ₄₂ (Figure 3C,D).

2.6. Brain Soluble Aβ, IgG Extravasation, and Sleep Correlation

We performed the Spearman correlation analysis to clarify the relationship between brain soluble Aβ, IgG extravasation, and total sleep hours and whether the correlation is significant. As shown in Figure 4, and as expected, a positive correlation with Spearman *R* = 0.6736 (*p* = 0.004) between brain soluble Aβ levels and IgG extravasation was observed, supporting Aβ contribution to BBB breakdown. In addition, an inverse correlation between total sleep time and IgG extravasation was also observed (Spearman *R* = −0.8546;

$p < 0.0001$); however, a weak correlation between brain soluble A β and sleep time was observed with Spearman $R = -0.3218$ ($p = 0.0949$).

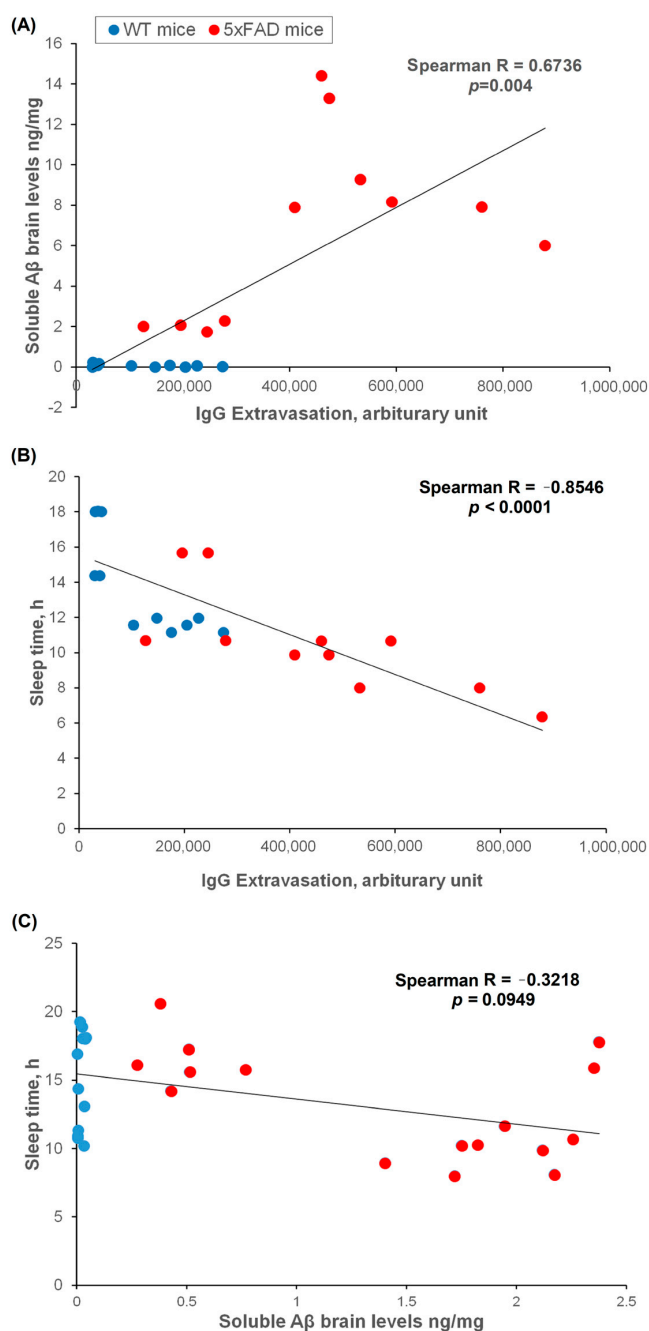


Figure 4. Correlation analysis between IgG extravasation and soluble brain A β levels (A) and sleep time (B), and between soluble brain A β and sleep time (C). For A and B, $n = 11$ mice/group were used; for C, $n = 16$ mice/group were used.

2.7. Effect of OC Treatment on Metabolic Phenotypes, A β , and Related Pathology

In young 5xFAD-4m mice (Figure 5), the daily treatment with OC (10 mg/kg) by oral gavage for 3 months significantly altered metabolic parameters. OC significantly increased food and water intake during the daytime compared to vehicle-treated 5xFAD mice without altering the body weight (Figure 5A–C). In addition, compared to vehicle-treated 5xFAD mice, mainly at nighttime, OC significantly reduced EE, VCO₂, VO₂, and RER to levels comparable to WT mice (Figure 5D–G). This effect was associated with an increased rate of water loss (VH₂O) during the daytime and nighttime to levels similar

to WT-4 m (Figure 5H) and significantly reduced movement and increased sleep time at nighttime to levels comparable to WT-4m mice (Figure 5I,K). Interestingly, the effect of OC treatment on the older 5xFAD mice (9 months) was more prominent. While OC increased 5xFAD-9m mice body weights by 4.0 g, the effect did not reach a significant effect compared to 5xFAD vehicle-treated mice; however, they were comparable to WT mice (Figure 6A). In addition, OC treatment significantly increased daytime and nighttime sleep hours by 1.4 and 1.2 h, respectively, approaching WT-9m mice (Figure 6K); OC treatment significantly reduced EE, VCO₂, VO₂, RER, distance traveled, and accumulative distance traveled almost to levels similar to those obtained with WT-9-month-old mice (Figure 6D–J), without altering food and water intake (Figure 5B,C). Changes in metabolic parameters suggest OC ameliorated parameters related to anxiety-linked behavior and sleep.

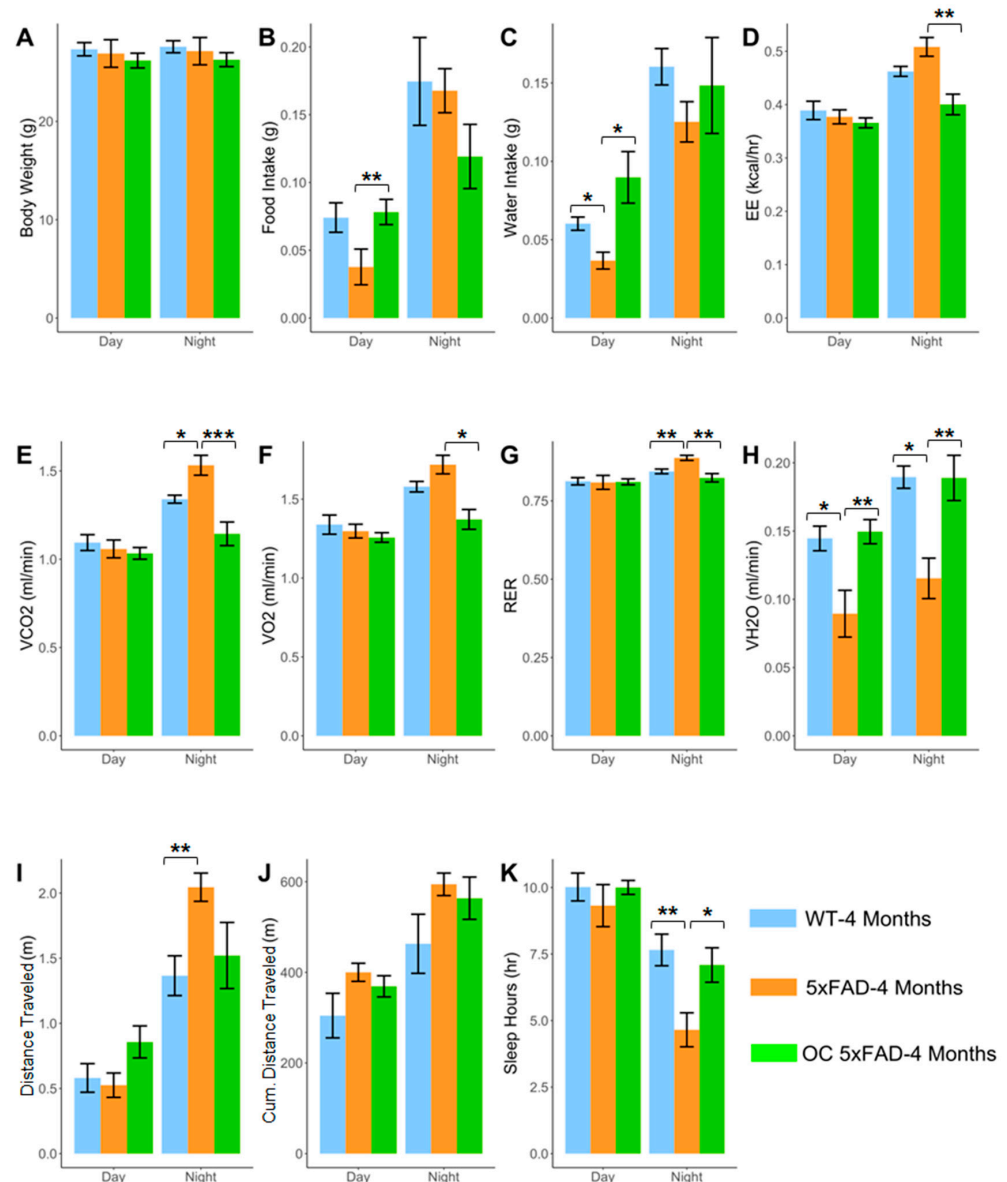


Figure 5. The effect of OC (10 mg/kg; PO) on the metabolic parameters (A) Body weight (g), (B) Food intake (g), (C) Water intake (g), (D) EE (kcal/h), (E) VCO₂ (mL/min), (F) VO₂ (mL/min), (G) RER, (H) VH₂O (mL/min), (I) Distance traveled (m), (J) Cumulative (Cum.) distance traveled (m), and (K) Sleep hours (h) in 4-month-old WT and 5xFAD mice at daytime and nighttime. Data are presented as mean \pm SEM for $n = 10$ mice/group. * $p < 0.05$, ** $p < 0.01$, and *** $p < 0.001$.

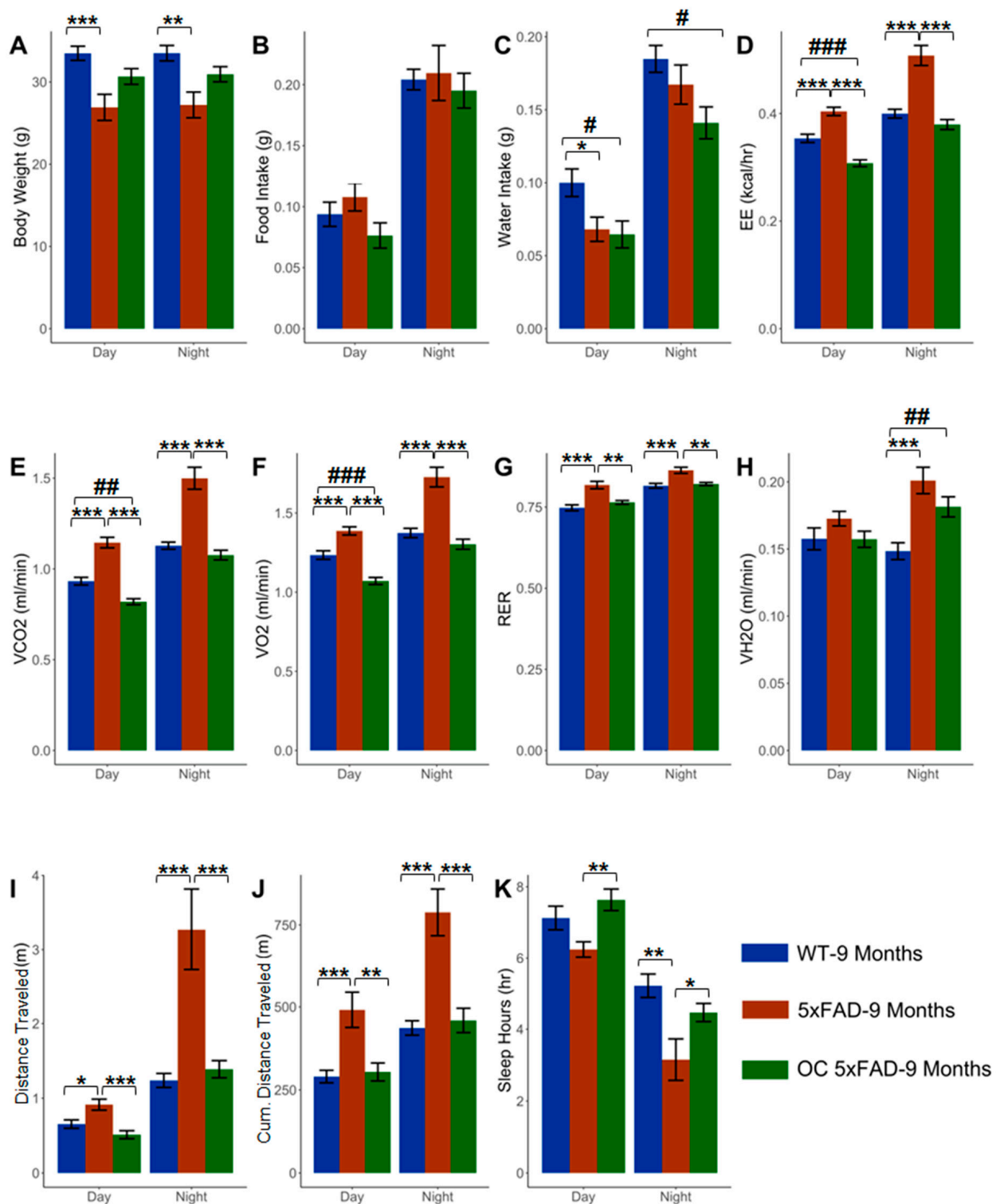


Figure 6. The effect of OC (10 mg/kg; PO) on the metabolic parameters (A) Body weight (g), (B) Food intake (g), (C) Water intake (g), (D) EE (kcal/h), (E) VCO₂ (mL/min), (F) VO₂ (mL/min), (G) RER, (H) VH₂O (mL/min), (I) Distance traveled (m), (J) Cumulative (Cum.) distance traveled (m), and (K) Sleep hours (h) in 9-month-old WT and 5xFAD mice at daytime and nighttime. Data are presented as mean ± SEM for *n* = 10 mice/group. * *p* < 0.05, ** *p* < 0.01, *** *p* < 0.001, # *p* < 0.05, ## *p* < 0.01, and ### *p* < 0.001.

For OC effect on A β plasma and brain levels, as shown in Figure 3, OC-treated 5xFAD-4m mice demonstrated a significantly reduced plasma A β ₄₀ and A β ₄₂ by 67% and 52%

approaching WT-4m levels, while increased their levels in 5xFAD-9m by 1.66- and 1.56-fold approaching the WT-9m levels. In the brain, OC significantly reduced $A\beta_{40}$ by 40% and 73% in 4- and 9-month-old mice, respectively, and $A\beta_{42}$ levels by 45% in 9-month-old 5xFAD mice. This effect was associated with a noticeable significant reduction in IgG extravasation (Figure 2), which is consistent with our previous results [27,28].

3. Discussion

Aging and AD alter body metabolism [30,31], which could be modulated by lifestyle changes and therapeutic treatments. The objectives of this work were to (1) assess changes in metabolic and behavior phenotypic parameters with age and AD pathology in WT and 5xFAD mice; (2) associate sleep disturbances with BBB dysfunction and $A\beta$ brain levels; and (3) evaluate the effect of pathology modulation by OC treatment on the metabolic and behavior parameters. Our findings demonstrate metabolic and behavioral alterations in WT and 5xFAD mouse models with age and pathology. The findings also revealed a correlation between BBB leakage and brain soluble $A\beta$ levels and, for the first time, a correlation between BBB leakage and sleep time. In addition, 5xFAD mice treatment with OC modulated metabolic and behavioral parameters, with a more prominent effect in the older 5xFAD mice.

AD patients have lower body weight than cognitively normal individuals of the same age due to appetite and metabolic state changes [6,32]. In addition, dehydration is one of the symptoms induced in AD patients [33]. In our studies in mice, we observed that 5xFAD-9m mice have lower body weight than WT-9m, although food intake was the same in both strains. The reduced body weight at an older age could be related to the general increase in body metabolism represented by the increased dehydration rate (parameter VH_2O), hyperventilation (parameters VO_2 , VCO_2 , and RER), activity rate (parameter EE), movement (traveled distance), and sleep disturbances, all of which could be associated with anxiety-like behavior in mice.

With normal aging in WT mice, we observed a decreased activity, metabolism, and movement, which is in contrast to the effect in 5xFAD mice where a higher activity and metabolism with greater movement was determined, suggesting $A\beta$ and related pathology in 5xFAD mice is contributing to the observed effect, thus to the anxiety-like behavior. Previous assessments of anxiety-like behavior in mouse models of AD demonstrated inconsistent and contradictory results. For example, in some studies, 5xFAD and APP/PS1 mice exhibited decreased or equivalent anxiety-like behavior in the open field or elevated plus maze relative to WT mice [34–36]. On the other hand, others have reported increased anxiety-like behavior in 5xFAD mice and other AD mouse models [37–39]. Such inconsistencies in the results could be related to the experimental conditions. For example, the elevated plus-maze tests are frequently used to assess mouse anxiety by locating them at a specific height, which introduces a fear factor by exposing them to the open and height, while the phenotypic behavior monitored in this work is fear-free. The mouse anxiety assessment was performed in the home cage under standard housing conditions, which is more similar to that in humans. Indeed, additional studies are necessary to correlate the anxiety-like behavior determined from the metabolic and behavior parameters with those determined using open field and elevated plus-maze tests under the same experimental conditions.

Furthermore, with aging, the elderly experience a sleep–wake disruption induced by physiological changes, such as aging, or due to the presence of a disease condition [40]. The elderly tend to have more frequency of taking light sleep than deep sleep, suggesting a less efficient circadian behavior [40]. Sleep disturbance is considered one of the well-known behavioral phenotypes of AD [41], which worsens as the disease progresses [8,42]. The progressive neuropathological alteration and $A\beta$ burden in AD have been associated with sleep dysregulation, thus impacting the sleep–wake activity [42–44]. When tested in WT mice, the cerebral injection of $A\beta_{25-35}$ significantly reduced non-rapid eye movement sleep and increased wakefulness [45,46], suggesting a role for $A\beta$ in sleep disturbances. With aging, we observed that the 9-month-old WT mice have reduced sleep time compared to

the 4-month-old young mice. These findings are consistent with those reported by Soltani and colleagues, who assessed the effect of aging on the sleep–wake cycle and concluded that the induced sleep disorder in 12-month-old C57BL/6 mice was comparable to that in 3-month-old mice [47]. In the AD mouse model, 5xFAD mice also exhibited a significantly reduced sleeping time at both ages compared to the WT mice supporting that in AD, besides aging, the sleep pattern is influenced by A β pathology.

To correlate changes in metabolic and behavioral phenotypes with A β and related pathology as a function of age and pathology, we assessed plasma and brain A β levels and the BBB function. As the disease progressed with age, the accumulation of A β increased in the 5xFAD mouse brains. However, in plasma, while the low A β levels were not significantly altered in the WT mice with age, in 5xFAD mice, the plasma levels of A β were significantly higher in 4-month-old compared to 9-month-old mice. Neurotoxic agents, such as A β , are cleared, at least in part, from the brain to the blood across the BBB [48]. At 4 months of age, the higher plasma levels of A β in 5xFAD than WT could be due to the increased production of brain A β that gets cleared to the blood across the BBB [49,50]. In contrast, the reduced A β plasma levels in 5xFAD-9m mice relative to 5xFAD 4-m and WT-9m mice could be explained, at least in part, by reduced A β clearance across the BBB and its brain accumulation. In AD, as the disease progresses, the elimination of A β is reduced due to reduced degradation and clearance across the BBB, leading to brain A β accumulation and plaque formation [49–51]. In AD mouse models, increased brain A β is associated with BBB breakdown supported by the increased IgG extravasation, which significantly increased as the disease progressed. Our correlation studies showed a positive correlation between brain A β and IgG extravasation and a negative correlation between total sleep hours and IgG extravasation, which suggests the association of BBB breakdown with reduced sleep time, an effect that is mediated by A β ; however, the correlation between soluble A β and sleep hours was not strong. Indeed, additional studies are required to explain these findings.

To assess the effect of AD treatment on the metabolic and behavior parameters and whether they can be rectified, we used the phenolic compound oleocanthal (OC) as a model molecule. We previously reported that OC at 5 and 10 mg/kg doses demonstrates a protective and therapeutic effect against A β and related pathology in AD mouse models [25–28]. In addition, we also reported that OC crosses the BBB, where we detected it in mouse brains following an intravenous administration [52]. In the current study, 5xFAD mice treatment with 10 mg/kg OC modulated the metabolic and behavior parameters to values approaching the WT mice, with the effect being more pronounced in the 9-month-old than the 4-month-old 5xFAD mice. OC treatment increased the body weight of mice, which could be explained, at least in part, by the reduced activity rate and anxiety-like behavior. OC also improved sleeping time during the day to values comparable to the WT mice of the same age suggesting its beneficial effect against anxiety and sleep disturbances. This observed effect with OC was associated with reduced brain A β levels and improved BBB function. The effect of OC on plasma A β levels differed between 5xFAD-4m (i.e., early disease stage) and 5xFAD-9m (i.e., with advanced pathology), where OC reduced plasma A β in the former and increased it in the latter. Indeed, additional studies are necessary to explain these results; however, we speculate that the dysregulated balance between A β production and clearance, and the difference in this dysregulation between early and advanced pathology influenced the effect of OC. For example, vehicle-treated 5xFAD-4m mice demonstrated higher plasma A β levels than 5xFAD-9m mice, suggesting the better clearance of produced soluble A β to the blood across the BBB. However, as the pathology advances, at 9 months and due to increased aggregation and deposition of produced A β in the form of plaques, the reduced available soluble A β for clearance across the dysfunctional BBB could impact A β plasma levels, which collectively were rectified by OC treatment. We previously reported that OC reduces brain A β production and increases its clearance across the BBB [26,50,53], which, thus, could explain the observed effect.

This study has several limitations, notably the use of male WT and 5xFAD mice and not including female mice, which require evaluation. Besides, additional studies using conventional tasks such as the open field test could be necessary to confirm the anxiety-like behavior and its reduction by OC treatment, which are planned for future investigation. Furthermore, additional studies are required to confirm and explain our correlation studies, including the correlation between sleep and soluble A β , as well as with total A β (soluble and insoluble).

In conclusion, we observed metabolic and behavioral alterations with age and pathology in WT and 5xFAD mouse models. With aging, 5xFAD mice demonstrate a reduced body weight, increased metabolic activity rate, and increased anxiety-like behavior, opposite to those observed in WT mice. In addition, both mouse models demonstrated reduced sleep hours, with 5xFAD mice showing less sleeping time than WT mice. Our findings also reveal a relationship between reduced sleep duration and BBB breakdown for the first time. Furthermore, 5xFAD mice treatment with OC ameliorated the assessed metabolic and behavior parameters. OC improved anxiety-like behavior symptoms and increased sleeping hours, two major symptoms of AD. In conclusion, our findings indicate that the metabolic and behavioral parameters assessed in this study could be used as assessment tools for disease progression, severity, and treatment efficacy in mouse models of AD.

4. Materials and Methods

4.1. Animals

Male wild-type C57BL/6J (Strain #:000664) and 5xFAD (Strain #: 034848-JAX; both from Jackson Laboratory, Bar Harbor, ME, USA) mouse models were used in the studies at 4 and 9 months of age ($n = 10$ mice per group). In addition to these four groups, other two groups were added ($n = 10$ mice/group), namely, 5xFAD-4-month-old and 5xFAD-9-month-old that received 10 mg/kg OC by oral gavage daily for 3 months starting at the age of 1 and 6 months, respectively. WT and 5xFAD mice received saline (as a vehicle) by oral gavage. OC is an amphiphilic compound and is water soluble [54]. A schematic diagram of the experimental design is demonstrated in Scheme 1. The AD mouse model 5xFAD expresses human amyloid precursor protein (APP) with the mutations APP KM670/671NL (Swedish), APP I716V (Florida), APP V717I (London), and PSEN1 M146L and PSEN1 L286V, leading to early and aggressive A β accumulation associated with deficits in spatial learning as the disease progresses [55]. In 5xFAD mice, extracellular A β plaque deposition starts at 2 months with gliosis. This early A β deposition and gliosis induce synaptic loss, resulting in cognitive impairment at 4 months. Aged C57BL/6J mice are frequently used in studies related to neurodegenerative disorders. C57BL/6 mice demonstrate a decline in physical function as early as 6 months of age, while the cognitive function begins to decline later, with a considerable impairment present at 22 months of age [56]. WT and 5xFAD mice were housed for breeding in plastic containers under 12 h light/dark cycle, 22 °C, 35% relative humidity, and *ad libitum* access to water and food. At 4 and 9 months of age, mice were transferred to metabolic cages as described below to perform the metabolic and behavioral phenotypes assessments. All animal experiments and procedures were approved by the Institutional Animal Care and Use Committee of Auburn University and according to the National Institutes of Health Guidelines Principles of Laboratory Animal Care.

4.2. Metabolic and Behavioral Phenotyping Assessments

Promethion metabolic mouse cages (Sable Systems, Las Vegas, NV, USA) were used to house animals for metabolic screening and phenotyping. Animals were transferred from their home cages and singly housed in the metabolic cages at 4 and 9 months of age. The animals were housed in the metabolic cages for 36 h, with the first 12 h stated for the cage environment adaptation and the next 24 h for data collection. Animal activity was measured using Promethion XYZ Beambreak Activity Monitor. Food and water intake, body weight, movement distance, sleeping time, VO $_2$, and VCO $_2$ were measured using Promethion precision MM-1 Load Cell Sensors. The time for metabolic parameters

measurement is defined as 12h:12h light:dark cycle with ZT 0 (representing lights on) and ZT12 (representing lights off). The amount of food and water withdrawn from the container was measured and analyzed. The body weight monitors were plastic tubes that also function as in-cage enrichment and nesting devices. VH_2O , VCO_2 , and VO_2 (all measured in mL/min) were analyzed using the Promethion GA-3 gas analyzer to provide detailed respirometry data. Mean energy expenditure (EE) was calculated in kilocalories/hour (kcal/h) by utilizing the Weir equation: $60 \times (0.003941 \times VO_2 (n) + 0.001106 \times VCO_2 (n))$. ANCOVA was used to adjust for the influence of body weight as a covariate on EE and VO_2 using custom R scripts based on the multiple linear regression analysis described on the MMPC Energy Expenditure analysis page [57]. RER was determined by measuring gas exchange within the metabolic cages to identify the substrate primarily utilized for energy within the body. Specifically, RER is the ratio of VCO_2 produced to VO_2 ($RER = VCO_2/VO_2$). All metabolic phenotyping data were analyzed using ExpeData software (version 1.8.2; Sable Systems) with Universal Macro Collection (version 10.1.3; Sable Systems). The parameter distance traveled is the sum of all distances traveled within the beam break system in meters (m), including fine movement (such as grooming and scratching) and direct locomotion.

4.3. Immunofluorescence Staining

After the phenotyping assessment, mice were sacrificed to collect the blood and brain tissues. Brain sections of 15 μ m were prepared using a ThermoScientific HM525 NX Cryostat (Waltham, MA, USA). Sections were fixed with 4% paraformaldehyde and then blocked with the blocking buffer TrueBlack background suppressor (Biotum; Fremont, CA, USA) for 60 min. IgG extravasation from brain microvessels was determined to assess BBB integrity. For this, sections were probed using dual immunohistochemical staining with anti-rabbit collagen-IV as the primary antibody to detect brain microvessels (Millipore Sigma, Burlington, MA, USA) and Alexa Fluor[®] 488-conjugated goat anti-mouse IgG H&L (Abcam, Cambridge, UK) to detect IgG extravasation, both at 1:500 dilution. The secondary antibody for collagen-IV antibody was anti-rabbit (Alexa Fluor[®] 594) (Abcam). For each treatment, image acquisition was performed in 10 tissue sections spanning the hippocampus and cortex, each separated by 150 μ m (total of 20 sections per mouse). Images were captured and adjusted to the lowest background signal using Nikon Eclipse Ti-S inverted fluorescence microscope (Melville, NY, USA). To quantify IgG extravasation, sections were normalized to the same background. Images were analyzed using Image J software (National Institutes of Health, Bethesda, MD, USA) that was set for mean value, minimum value, maximum value, and limit of the threshold followed by analysis.

4.4. Measurements of Brain and Plasma $A\beta$ Using ELISA

Commercially available ELISA kits were used to determine $A\beta_{40}$ and $A\beta_{42}$ levels in WT and 5xFAD mice brain tissue lysates and plasma according to the manufacturer's instructions (R&D Systems, Minneapolis, MN, USA). All samples were run in duplicate. Brain $A\beta$ levels were corrected to the total protein amount in each sample using the bicinchoninic acid (BCA) assay.

4.5. Statistical Analysis

All metabolic phenotype parameters were analyzed with RStudio and the R_{x64} 3.6.0 software environment (RStudio, PBC, Boston, MA, USA). Twenty-four-hour circadian data were analyzed using the random-effects model to account for the repeated measures from an individual animal. A one-way ANOVA test with *Tukey post hoc* using GraphPad Prism (San Diego, CA, USA) was used to evaluate the difference between the three groups. Student's *t*-test was used to evaluate differences between the two groups. The nonparametric Spearman correlation with a two-tailed *p*-value is used for the correlation analysis. Significance for all measures was determined at $p < 0.05$, and all data are presented as mean \pm SEM.

Supplementary Materials: The following supporting information can be downloaded at: <https://www.mdpi.com/article/10.3390/molecules28145592/s1>, Figure S1: The effect of aging on changes in metabolic parameters in 4- vs. 9-month-old WT mice with time for 24 h. Data are presented as mean \pm SEM for n = 10 mice/group for each time point; Table S1: Statistical significance of WT-4 vs. WT-9 months shown in Figure S1; Figure S2: The effect of aging on changes in metabolic parameters in 4- vs. 9-month-old 5xFAD mice with time for 24 h. Data are presented as mean \pm SEM for n = 10 mice/group for each time point; Table S2: Statistical significance of 5xFAD-4 vs. 5xFAD-9 months shown in Figure S2; Figure S3: The effect of pathology on changes in metabolic parameters in 4-months old WT vs. 5xFAD mice with time for 24 h. Data are presented as mean \pm SEM for n = 10 mice/group for each time point; Table S3: Statistical significance of 4 months WT vs. 5xFAD in Figure S3; Figure S4: The effect of pathology on changes in metabolic parameters in 9-months old WT vs. 5xFAD mice with time for 24 h. Data are presented as mean \pm SEM for n = 10 mice/group for each time point; Table S4: Statistical significance of 9 months WT vs. 5xFAD in Figure S4.

Author Contributions: E.Y. performed the experiments and data analysis and wrote the manuscript; J.W. and L.N.W. performed the experiments, analyzed data, and reviewed the manuscript; M.W.G. performed data analysis and reviewed and edited the manuscript; A.K. contributed to designing the experiments, writing, reviewing, and editing the manuscript, and funding acquisition. All authors have read and agreed to the published version of the manuscript.

Funding: This research was funded by Auburn University Intramural Grants Program (IGP; to Amal Kaddoumi), by the National Institute of Aging (NIH/NIA) under grant number R43AG061952 (Amal Kaddoumi with Oleolive, LLC), and by the National Institute of Neurological Disorders and Stroke (NIH/NINDS; to Amal Kaddoumi) under grant number R21NS101506.

Institutional Review Board Statement: The study was conducted according to the guidelines of the Declaration of Helsinki and approved by the Institutional Animal Care and Use Committee of Auburn University (protocol code 2018-3388, date of approval 11 September 2018).

Informed Consent Statement: Not Applicable.

Data Availability Statement: The data supporting this paper and other study findings are available from the corresponding author upon reasonable request.

Conflicts of Interest: The authors declare no conflict of interest. The corresponding author, Amal Kaddoumi, is a co-founder and equity shareholder in Oleolive, LLC. The funders had no role in the study's design; in the collection, analyses, or interpretation of data; in the writing of the manuscript, or in the decision to publish the results.

Sample Availability: Not Applicable.

References

1. Jafari Nasabian, P.; Inglis, J.E.; Reilly, W.; Kelly, O.J.; Ilich, J.Z. Aging human body: Changes in bone, muscle and body fat with consequent changes in nutrient intake. *J. Endocrinol.* **2017**, *234*, R37–R51. [[CrossRef](#)] [[PubMed](#)]
2. Holmes, E.; Loo, R.L.; Stamler, J.; Bictash, M.; Yap, I.K.; Chan, Q.; Ebbels, T.; De Iorio, M.; Brown, I.J.; Veselkov, K.A.; et al. Human metabolic phenotype diversity and its association with diet and blood pressure. *Nature* **2008**, *453*, 396–400. [[CrossRef](#)] [[PubMed](#)]
3. Luo, Y.; Burrington, C.M.; Graff, E.C.; Zhang, J.; Judd, R.L.; Suksaranjit, P.; Kaewpoowat, Q.; Davenport, S.K.; O'Neill, A.M.; Greene, M.W. Metabolic phenotype and adipose and liver features in a high-fat Western diet-induced mouse model of obesity-linked NAFLD. *Am. J. Physiol. Endocrinol. Metab.* **2016**, *310*, E418–E539. [[CrossRef](#)]
4. Di Iulio, F.; Palmer, K.; Blundo, C.; Casini, A.R.; Gianni, W.; Caltagirone, C.; Spalletta, G. Occurrence of neuropsychiatric symptoms and psychiatric disorders in mild Alzheimer's disease and mild cognitive impairment subtypes. *Int. Psychogeriatr.* **2010**, *22*, 629–640. [[CrossRef](#)]
5. Suma, S.; Watanabe, Y.; Hirano, H.; Kimura, A.; Edahiro, A.; Awata, S.; Yamashita, Y.; Matsushita, K.; Arai, H.; Sakurai, T. Factors affecting the appetites of persons with Alzheimer's disease and mild cognitive impairment. *Geriatr. Gerontol. Int.* **2018**, *18*, 1236–1243. [[CrossRef](#)] [[PubMed](#)]
6. Grundman, M.; Corey-Bloom, J.; Jernigan, T.; Archibald, S.; Thal, L.J. Low body weight in Alzheimer's disease is associated with mesial temporal cortex atrophy. *Neurology* **1996**, *46*, 1585–1591. [[CrossRef](#)]
7. Westerterp, K.R. Control of energy expenditure in humans. *Eur. J. Clin. Nutr.* **2017**, *71*, 340–344. [[CrossRef](#)]

8. Brzecka, A.; Leszek, J.; Ashraf, G.M.; Ejma, M.; Avila-Rodriguez, M.F.; Yarla, N.S.; Tarasov, V.V.; Chubarev, V.N.; Samsonova, A.N.; Barreto, G.E.; et al. Sleep Disorders Associated With Alzheimer's Disease: A Perspective. *Front. Neurosci.* **2018**, *12*, 330. [[CrossRef](#)]
9. Krueger, J.M.; Frank, M.G.; Wisor, J.P.; Roy, S. Sleep function: Toward elucidating an enigma. *Sleep. Med. Rev.* **2016**, *28*, 46–54. [[CrossRef](#)]
10. Lee, H.; Xie, L.; Yu, M.; Kang, H.; Feng, T.; Deane, R.; Logan, J.; Nedergaard, M.; Benveniste, H. The Effect of Body Posture on Brain Glymphatic Transport. *J. Neurosci.* **2015**, *35*, 11034–11044. [[CrossRef](#)]
11. Mendelsohn, A.R.; Larrick, J.W. Sleep facilitates clearance of metabolites from the brain: Glymphatic function in aging and neurodegenerative diseases. *Rejuvenation Res.* **2013**, *16*, 518–523. [[CrossRef](#)]
12. O'Donnell, J.; Ding, F.; Nedergaard, M. Distinct functional states of astrocytes during sleep and wakefulness: Is norepinephrine the master regulator? *Curr. Sleep. Med. Rep.* **2015**, *1*, 1–8. [[CrossRef](#)]
13. Xie, L.; Kang, H.; Xu, Q.; Chen, M.J.; Liao, Y.; Thiyagarajan, M.; O'Donnell, J.; Christensen, D.J.; Nicholson, C.; Iliff, J.J.; et al. Sleep drives metabolite clearance from the adult brain. *Science* **2013**, *342*, 373–377. [[CrossRef](#)] [[PubMed](#)]
14. Carvalho, D.Z.; St. Louis, E.K.; Knopman, D.S.; Boeve, B.F.; Lowe, V.J.; Roberts, R.O.; Mielke, M.M.; Przybelski, S.A.; Machulda, M.M.; Petersen, R.C.; et al. Association of Excessive Daytime Sleepiness With Longitudinal beta-Amyloid Accumulation in Elderly Persons Without Dementia. *JAMA Neurol.* **2018**, *75*, 672–680. [[CrossRef](#)] [[PubMed](#)]
15. Ju, Y.E.; McLeland, J.S.; Toedebusch, C.D.; Xiong, C.; Fagan, A.M.; Duntley, S.P.; Morris, J.C.; Holtzman, D.M. Sleep quality and preclinical Alzheimer disease. *JAMA Neurol.* **2013**, *70*, 587–593. [[CrossRef](#)] [[PubMed](#)]
16. Masule, M.V.; Rathod, S.; Agrawal, Y.; Patil, C.R.; Nakhate, K.T.; Ojha, S.; Goyal, S.N.; Mahajan, U.B. Ghrelin mediated regulation of neurosynaptic transmitters in depressive disorders. *Curr. Res. Pharmacol. Drug Discov.* **2022**, *3*, 100113. [[CrossRef](#)] [[PubMed](#)]
17. Gimson, A.; Schlosser, M.; Huntley, J.D.; Marchant, N.L. Support for midlife anxiety diagnosis as an independent risk factor for dementia: A systematic review. *BMJ Open* **2018**, *8*, e019399. [[CrossRef](#)]
18. Pentkowski, N.S.; Rogge-Obando, K.K.; Donaldson, T.N.; Bouquin, S.J.; Clark, B.J. Anxiety and Alzheimer's disease: Behavioral analysis and neural basis in rodent models of Alzheimer's-related neuropathology. *Neurosci. Biobehav. Rev.* **2021**, *127*, 647–658. [[CrossRef](#)]
19. Bobba, A.; Amadoro, G.; Valenti, D.; Corsetti, V.; Lassandro, R.; Atlante, A. Mitochondrial respiratory chain Complexes I and IV are impaired by β -amyloid via direct interaction and through Complex I-dependent ROS production, respectively. *Mitochondrion* **2013**, *13*, 298–311. [[CrossRef](#)]
20. Ferrer, I. Altered mitochondria, energy metabolism, voltage-dependent anion channel, and lipid rafts converge to exhaust neurons in Alzheimer's disease. *J. Bioenerg. Biomembr.* **2009**, *41*, 425–431. [[CrossRef](#)]
21. Zhu, Y.; Gao, M.; Huang, H.; Gao, S.-H.; Liao, L.-Y.; Tao, Y.; Cheng, H.; Gao, C.-Y. p75NTR Ectodomain Ameliorates Cognitive Deficits and Pathologies in a Rapid Eye Movement Sleep Deprivation Mice Model. *Neuroscience* **2022**, *496*, 27–37. [[CrossRef](#)] [[PubMed](#)]
22. Han, S.M.; Jang, Y.J.; Kim, E.Y.; Park, S.A. The Change in Circadian Rhythms in P301S Transgenic Mice is Linked to Variability in Hsp70-related Tau Disaggregation. *Exp. Neurobiol.* **2022**, *31*, 196. [[CrossRef](#)]
23. Holth, J.K.; Mahan, T.E.; Robinson, G.O.; Rocha, A.; Holtzman, D.M. Altered sleep and EEG power in the P301S Tau transgenic mouse model. *Ann. Clin. Transl. Neurol.* **2017**, *4*, 180–190. [[CrossRef](#)] [[PubMed](#)]
24. Beauchamp, G.K.; Keast, R.S.; Morel, D.; Lin, J.; Pika, J.; Han, Q.; Lee, C.-H.; Smith, A.B.; Breslin, P.A. Ibuprofen-like activity in extra-virgin olive oil. *Nature* **2005**, *437*, 45–46. [[CrossRef](#)]
25. Batareseh, Y.S.; Mohamed, L.A.; Al Rihani, S.B.; Mousa, Y.M.; Siddique, A.B.; El Sayed, K.A.; Kaddoumi, A. Oleocanthal ameliorates amyloid-beta oligomers' toxicity on astrocytes and neuronal cells: In vitro studies. *Neuroscience* **2017**, *352*, 204–215. [[CrossRef](#)]
26. Qosa, H.; Batareseh, Y.S.; Mohyeldin, M.M.; El Sayed, K.A.; Keller, J.N.; Kaddoumi, A. Oleocanthal enhances amyloid-beta clearance from the brains of TgSwDI mice and in vitro across a human blood-brain barrier model. *ACS Chem. Neurosci.* **2015**, *6*, 1849–1859. [[CrossRef](#)] [[PubMed](#)]
27. Batareseh, Y.S.; Kaddoumi, A. Oleocanthal-rich extra-virgin olive oil enhances donepezil effect by reducing amyloid-beta load and related toxicity in a mouse model of Alzheimer's disease. *J. Nutr. Biochem.* **2018**, *55*, 113–123. [[CrossRef](#)]
28. Al Rihani, S.B.; Darakjian, L.I.; Kaddoumi, A. Oleocanthal-Rich Extra-Virgin Olive Oil Restores the Blood-Brain Barrier Function through NLRP3 Inflammasome Inhibition Simultaneously with Autophagy Induction in TgSwDI Mice. *ACS Chem. Neurosci.* **2019**, *10*, 3543–3554. [[CrossRef](#)]
29. Mehta, R.I.; Carpenter, J.S.; Mehta, R.I.; Haut, M.W.; Ranjan, M.; Najib, U.; Lockman, P.; Wang, P.; D'Haese, P.F.; Rezai, A.R. Blood-Brain Barrier Opening with MRI-guided Focused Ultrasound Elicits Meningeal Venous Permeability in Humans with Early Alzheimer Disease. *Radiology* **2021**, *298*, 654–662. [[CrossRef](#)]
30. Baum, J.I.; Kim, I.Y.; Wolfe, R.R. Protein Consumption and the Elderly: What Is the Optimal Level of Intake? *Nutrients* **2016**, *8*, 359. [[CrossRef](#)]
31. Pilgrim, A.L.; Robinson, S.M.; Sayer, A.A.; Roberts, H.C. An overview of appetite decline in older people. *Nurs. Older People* **2015**, *27*, 29–35. [[CrossRef](#)] [[PubMed](#)]
32. Wang, P.N.; Yang, C.L.; Lin, K.N.; Chen, W.T.; Chwang, L.C.; Liu, H.C. Weight loss, nutritional status and physical activity in patients with Alzheimer's disease. A controlled study. *J. Neurol.* **2004**, *251*, 314–320. [[CrossRef](#)] [[PubMed](#)]

33. Albert, S.G.; Nakra, B.R.; Grossberg, G.T.; Caminal, E.R. Vasopressin response to dehydration in Alzheimer's disease. *J. Am. Geriatr. Soc.* **1989**, *37*, 843–847. [[CrossRef](#)] [[PubMed](#)]
34. Arendash, G.W.; Gordon, M.N.; Diamond, D.M.; Austin, L.A.; Hatcher, J.M.; Jantzen, P.; DiCarlo, G.; Wilcock, D.; Morgan, D. Behavioral assessment of Alzheimer's transgenic mice following long-term Abeta vaccination: Task specificity and correlations between Abeta deposition and spatial memory. *DNA Cell Biol.* **2001**, *20*, 737–744. [[CrossRef](#)]
35. Jawhar, S.; Trawicka, A.; Jenneckens, C.; Bayer, T.A.; Wirths, O. Motor deficits, neuron loss, and reduced anxiety coinciding with axonal degeneration and intraneuronal Abeta aggregation in the 5XFAD mouse model of Alzheimer's disease. *Neurobiol. Aging* **2012**, *33*, 196.e29–196.e40. [[CrossRef](#)]
36. Radde, R.; Bolmont, T.; Kaeser, S.A.; Coomaraswamy, J.; Lindau, D.; Stoltze, L.; Calhoun, M.E.; Jaggi, F.; Wolburg, H.; Gengler, S.; et al. Abeta42-driven cerebral amyloidosis in transgenic mice reveals early and robust pathology. *EMBO Rep.* **2006**, *7*, 940–946. [[CrossRef](#)]
37. Flanigan, T.J.; Xue, Y.; Kishan Rao, S.; Dhanushkodi, A.; McDonald, M.P. Abnormal vibrissa-related behavior and loss of barrel field inhibitory neurons in 5xFAD transgenics. *Genes. Brain Behav.* **2014**, *13*, 488–500. [[CrossRef](#)]
38. Lippi, S.L.P.; Smith, M.L.; Flinn, J.M. A Novel hAPP/htau Mouse Model of Alzheimer's Disease: Inclusion of APP with Tau Exacerbates Behavioral Deficits and Zinc Administration Heightens Tangle Pathology. *Front. Aging Neurosci.* **2018**, *10*, 382. [[CrossRef](#)]
39. Sterniczuk, R.; Antle, M.C.; Laferla, F.M.; Dyck, R.H. Characterization of the 3xTg-AD mouse model of Alzheimer's disease: Part 2. Behavioral and cognitive changes. *Brain Res.* **2010**, *1348*, 149–155. [[CrossRef](#)]
40. Gulia, K.K.; Kumar, V.M. Sleep disorders in the elderly: A growing challenge. *Psychogeriatrics* **2018**, *18*, 155–165. [[CrossRef](#)]
41. Bliwise, D.L. Sleep disorders in Alzheimer's disease and other dementias. *Clin. Cornerstone* **2004**, *6* (Suppl. 1A), S16–S28. [[CrossRef](#)] [[PubMed](#)]
42. Van Erum, J.; Van Dam, D.; De Deyn, P.P. Sleep and Alzheimer's disease: A pivotal role for the suprachiasmatic nucleus. *Sleep. Med. Rev.* **2018**, *40*, 17–27. [[CrossRef](#)]
43. Brown, B.M.; Rainey-Smith, S.R.; Bucks, R.S.; Weinborn, M.; Martins, R.N. Exploring the bi-directional relationship between sleep and beta-amyloid. *Curr. Opin. Psychiatry* **2016**, *29*, 397–401. [[CrossRef](#)]
44. Brown, B.M.; Rainey-Smith, S.R.; Villemagne, V.L.; Weinborn, M.; Bucks, R.S.; Sohrabi, H.R.; Laws, S.M.; Taddei, K.; Macaulay, S.L.; Ames, D.; et al. The Relationship between Sleep Quality and Brain Amyloid Burden. *Sleep.* **2016**, *39*, 1063–1068. [[CrossRef](#)] [[PubMed](#)]
45. Cordone, S.; Annarumma, L.; Rossini, P.M.; De Gennaro, L. Sleep and beta-Amyloid Deposition in Alzheimer Disease: Insights on Mechanisms and Possible Innovative Treatments. *Front. Pharmacol.* **2019**, *10*, 695. [[CrossRef](#)] [[PubMed](#)]
46. Liu, Z.; Wang, F.; Tang, M.; Zhao, Y.; Wang, X. Amyloid beta and tau are involved in sleep disorder in Alzheimer's disease by orexin A and adenosine A(1) receptor. *Int. J. Mol. Med.* **2019**, *43*, 435–442. [[PubMed](#)]
47. Soltani, S.; Chauvette, S.; Bukhtiyarova, O.; Lina, J.M.; Dube, J.; Seigneur, J.; Carrier, J.; Timofeev, I. Sleep-Wake Cycle in Young and Older Mice. *Front. Syst. Neurosci.* **2019**, *13*, 51. [[CrossRef](#)]
48. Lopez, O.L.; Kuller, L.H.; Mehta, P.D.; Becker, J.T.; Gach, H.M.; Sweet, R.A.; Chang, Y.F.; Tracy, R.; DeKosky, S.T. Plasma amyloid levels and the risk of AD in normal subjects in the Cardiovascular Health Study. *Neurology* **2008**, *70*, 1664–1671. [[CrossRef](#)]
49. Deane, R.; Bell, R.D.; Sagare, A.; Zlokovic, B.V. Clearance of amyloid-beta peptide across the blood-brain barrier: Implication for therapies in Alzheimer's disease. *CNS Neurol. Disord. Drug Targets* **2009**, *8*, 16–30. [[CrossRef](#)]
50. Abuznait, A.H.; Qosa, H.; Busnena, B.A.; El Sayed, K.A.; Kaddoumi, A. Olive-oil-derived oleocanthal enhances beta-amyloid clearance as a potential neuroprotective mechanism against Alzheimer's disease: In vitro and in vivo studies. *ACS Chem. Neurosci.* **2013**, *4*, 973–982. [[CrossRef](#)]
51. Mohamed, L.A.; Keller, J.N.; Kaddoumi, A. Role of P-glycoprotein in mediating rivastigmine effect on amyloid-beta brain load and related pathology in Alzheimer's disease mouse model. *Biochim. Biophys. Acta* **2016**, *1862*, 778–787. [[CrossRef](#)]
52. Darakjian, L.I.; Rigakou, A.; Brannen, A.; Qusa, M.H.; Tasiakou, N.; Diamantakos, P.; Reed, M.N.; Panizzi, P.; Boersma, M.D.; Melliou, E. Spontaneous In Vitro and In Vivo Interaction of (–)-Oleocanthal with Glycine in Biological Fluids: Novel Pharmacokinetic Markers. *ACS Pharmacol. Transl. Sci.* **2021**, *4*, 179–192. [[CrossRef](#)] [[PubMed](#)]
53. Abdallah, I.M.; Al-Shami, K.M.; Alkhalifa, A.E.; Al-Ghraiya, N.F.; Guillaume, C.; Kaddoumi, A. Comparison of Oleocanthal-Low EVOO and Oleocanthal against Amyloid- β and Related Pathology in a Mouse Model of Alzheimer's Disease. *Molecules* **2023**, *28*, 1249. [[CrossRef](#)] [[PubMed](#)]
54. Siddique, A.B.; Ebrahim, H.; Mohyeldin, M.; Qusa, M.; Batarseh, Y.; Fayyad, A.; Tajmim, A.; Nazzal, S.; Kaddoumi, A.; El Sayed, K. Novel liquid-liquid extraction and self-emulsion methods for simplified isolation of extra-virgin olive oil phenolics with emphasis on (–)-oleocanthal and its oral anti-breast cancer activity. *PLoS ONE* **2019**, *14*, e0214798. [[CrossRef](#)]
55. Oakley, H.; Cole, S.L.; Logan, S.; Maus, E.; Shao, P.; Craft, J.; Guillozet-Bongaarts, A.; Ohno, M.; Disterhoft, J.; Van Eldik, L. Intraneuronal β -amyloid aggregates, neurodegeneration, and neuron loss in transgenic mice with five familial Alzheimer's disease mutations: Potential factors in amyloid plaque formation. *J. Neurosci.* **2006**, *26*, 10129–10140. [[CrossRef](#)] [[PubMed](#)]

56. Yanai, S.; Endo, S. Functional Aging in Male C57BL/6J Mice Across the Life-Span: A Systematic Behavioral Analysis of Motor, Emotional, and Memory Function to Define an Aging Phenotype. *Front. Aging Neurosci.* **2021**, *13*, 697621. [[CrossRef](#)] [[PubMed](#)]
57. Kaiyala, K.J.; Spiekerman, C.F.; Podolsky, R.H.; McGuinness, O. MMPC Energy Expenditure Analysis Page. Available online: <https://www.mmpc.org/shared/regression.aspx> (accessed on 27 April 2023).

Disclaimer/Publisher's Note: The statements, opinions and data contained in all publications are solely those of the individual author(s) and contributor(s) and not of MDPI and/or the editor(s). MDPI and/or the editor(s) disclaim responsibility for any injury to people or property resulting from any ideas, methods, instructions or products referred to in the content.